Asian Journal of Civil Engineering (2023) 24:639–655
https://doi.org/10.1007/s42107-022-00541-w

ORIGINAL PAPER

Effect of transverse opening on the strength of reinforced concrete column

Hailu Beza[1] · Goshu Kenea[2]

Received: 25 February 2022 / Accepted: 9 November 2022 / Published online: 6 December 2022

Abstract

Transverse openings may have been provided in reinforced concrete columns for the passage of services like plumbing pipes and electric conduits. These openings influence the behavior and strength of RC columns. Thus, it is important to study the effects of transverse opening on its behavior. This study focused on the strength of RC column with transverse opening by considering different opening ratios, the position of opening (at 0.25H, 0.5H, and 0.75H from the top end), concrete strength, loading eccentricity, and direction of loading eccentricity (when eccentricity parallel and normal to the longitudinal axis of transverse opening) as study parameters to access their effect on the ultimate strength, load versus vertical displacement curve and damage mode of column model. Fifty-four model specimens were selected, which are modeled with the concrete-damaged plasticity model in Abaqus 6.14. The FE model was validated against a previously conducted experimental investigation, which showed a good agreement with the experimental result. The study confirmed the significant effect of study parameters on the ultimate strength of the RC column. Further, a sensitivity analysis was performed to see how much the independent variables affect the ultimate strength of the column.

Keywords Opening ratio · Eccentricity · Direction of loading eccentricity · Ultimate strength · Damage mode · Position of opening

Abbreviations

CFRP	Carbon-Fiber-Reinforced-Polymers
w	Crack opening displacement
w_c	Crack opening displacement at which stress can no longer be transferred
c_1	Material constant equal to 3
c_2	Material constant equal to 3.93
G_F	Fracture or crushing energy
e_{po}	Eccentricity ratio (when the eccentricity is parallel to the opening)
e_{no}	Eccentricity ratio (when the eccentricity is perpendicular to the opening)
f_{ck}	Cylindrical compressive strength
Ecm	Concrete mean elastic modulus
f_{ctm}	Peak concrete tensile stress
f_{cm}	Mean compressive strength
P_{ult}	Ultimate load capacity
$\varnothing_r$	Opening ratio
l_{po}	Position of the opening
FE	Finite element

✉ Goshu Kenea
goshukeneatujuba@gmail.com

Hailu Beza
hailubeza11@gmail.com

[1] Civil Engineering Department, College of Engineering and Technology, Bule Hora University, Bule Hora, Oromia, Ethiopia

[2] Civil Engineering Department, Jimma Institute of Technology, Jimma University, Jimma, Oromia, Ethiopia

Introduction

Reinforced concrete columns are widely used structural members that carry loads mainly in compression and are designed to transfer loads from superstructures and finally to the soil through the foundations. Transverse openings may be present in reinforced concrete columns for the passage of services like sanitary reasons, ventilation, heating, air conditioning, and electrical ducts, and their presence is advantageous in terms of the economy and aesthetics of the buildings (Son et al., 2006). According to the ACI 318–14 (A. C. I., 2014) building code, conduits and pipes embedded within a column must not occupy more than 4% of the cross-sectional area on which strength is calculated.

Many formulations have been proposed in codes of practice or research documents to improve understanding of RC solid columns, both numerically (Gholipour et al., 2020; Ibrahim et al., 2015; Li et al., 2021; Raza et al., 2019) and experimentally (Hwang et al., 2020; Krainskyi et al., 2018; Hassan et al., 2013); K. T. A. Abdullah2., 2000; Landović & Bešević, 2021, Hwang et al., 2020; Balanji et al., 2016; (Zhang et al., 2017). A numerical investigation has been conducted on a partially loaded square column with high-strength concrete to access its ultimate strength and load versus vertical deflection by considering the effect of extra Carbon-Fiber-Reinforced-Polymers (CFRP) layers, loading eccentricity, and initial loading ratio as study parameters (Khelil et al., 2021). The study results confirmed a significant decrease in ultimate strength as initial loading and eccentricity increased. In addition, the performance of a RC column made from normal and high-strength concrete has been studied under monotonic and cyclic loading (Zarei, 2016). A column subjected to cyclic loading results in stiffness degradation. Furthermore, both numerical and experimental investigations were conducted on the reinforced concrete column made from recycled fine and coarse aggregate under compressive axial loading (Khelil, 2015). Both numerical and experimental results showed the same mode of damage.

Various studies (Isleem et al., 2021; Jiang & Wu, 2020; Waryosh et al., 2012; Othman & Mohammad, 2019) have been conducted on the behavior of reinforced concrete columns. The specimens were strengthened by different fiber-reinforced polymers under different loading eccentricities. The ultimate strength is increased as the ratio of fiber-reinforced polymer increases and loading eccentricity decreases. In another case, a numerical model was used to simulate the slender reinforced concrete column failure mode under different loading eccentricities (Rodrigues et al., 2015). Crushing of concrete in compression, yielding of steel rebar, and formation of cracks are taken into consideration, which is used to get the exact non-linear behavior of the model. The result concluded the significant effect of loading eccentricity on failure mode and cracking formation.

The most important parameters that govern the behavior of hollow columns are studied by Hoshikuma and Priestley (2000), in which axial load ratio, steel ratio, relative thickness ratio, and shape of the section are considered as study parameters. An experimental investigation (Bakhteri & Iskandar, 2005) and a numerical simulation (Al-Maliki et al., 2021) were performed to study the effect of an opening parallel to the longitudinal axis of the column cross-section under axial loading. Both studies testified to a significant reduction in axial load capacity due to the presence of openings as compared to a column with a solid section. Increasing longitudinal and transverse reinforcement was presented as a solution to strengthen the axial load capacity reduced by longitudinal opening.

Furthermore, an extensive experimental investigation was conducted on the ultimate strength of reinforced concrete columns with the presence of a transverse opening (I. A. S. AL-Shaarbaf et al., 2017). In the study, different opening ratios and loading eccentricity were considered to access the behavior of the RC column under axial loading. The study revealed a significant effect of opening ratio and loading eccentricity on the ultimate load capacity of the test specimens. Based on various literature reviews, studies on reinforced concrete columns with a transverse opening are very rare from the authors' knowledge. Therefore, the herein study aims to investigate the ultimate strength of RC column using numerical simulation with different transverse openings, different eccentricities, the direction of loading eccentricity, concrete strength, and position of the opening as study parameters. These transverse openings have different sizes, locations, and differences in shapes that can significantly affect the behavior and strength of the reinforced concrete columns. Numerically, no detailed investigations have been conducted into the different cases of transverse opening effects on the structural response of the reinforced concrete columns. Laboratory tests are labor-intensive, time-consuming, and costly. On the other hand, various empirical and code methods, based heavily on model test results, inevitably involve gross approximations that are not always reliable, and, by nature, their scope of applications is limited. Non-linear finite element analysis, however, provides an effective method by which structures can be analyzed to progressive failure. Non-linear analysis of concrete structures has become increasingly important and useful in recent years. In recent days, numerical analysis through finite element analysis software ABAQUS is attracting research areas due to its being faster, using modern computing techniques, easier, and more cost-effective than experimental study.

Research method

Concrete material modeling

The accuracy of a result obtained from FE simulation mainly depends on the accuracy of the stress–strain mathematical modeling used to represent the material non-linearity response. Data inputs from the concrete presented in Table 1 were used to model the specimens. The elastic modulus (E_{cm}) is computed based on the formula provided in Committee and for Standardization (2002), using cylindrical compressive strength (f_{ck}) as input. Concrete damage parameters were computed using mathematical equations and default values provided in Inc (2017) for both compressive and tensile stress behavior.

Table 1 Concrete compressive strengths used in the model

Concrete properties	Concrete grade				
	C-30.8	C-35	C-40	Poison's ratio	Density (kg/m3)
f_{ck} (MPa)	30.8	35	40	0.2	2400
E_{cm} (MPa)	33,042.45	34,077.15	35,220.46		

Concrete compressive behavior

It is not an easy task to establish an accurate stress relationship for concrete. To get concrete compressive stress–strain input data for modeling, the uniaxial concrete compressive stress–strain curve and equation provided in Committee and for Standardization (2002) were used. Up to about 30% of the maximum compressive strength, the uniaxial compressive stress–strain curve for concrete is assumed to be linearly elastic. Figure 1(a) shows the developed non-linear stress–strain response of C-30.8 concrete with uniaxial compressive loading.

Concrete tensile behavior

The tensile behavior can be defined by the yield stress as a function of displacement or strain to taken into account the tension stiffening effect (Committee & for Standardization, 2002; M. A. Yusuf Sümer*, 2015). When concrete cracks, some amount of load is transferred to reinforcement across cracks and carried by it. This effect is known as the tension stiffening effect, which is required in the concrete-damaged plasticity model as an input. It is specified through the post-failure stress-displacement relationship. An exponential function proposed in Karihaloo et al. (2003); H. W., 1986) was considered to extract input data for concrete tensile stress-displacement (as shown from Eqs. 1–3), which is the most accurate curve. Equation. 4 was employed to compute G_F (Alfarah et al., 2017). Figure 1(b) shows the developed non-linear tensile stress–strain response of C-30.8 concrete with uniaxial tensile loading.

$$\frac{\sigma}{f_{ctm}} = f(w) - \frac{w}{w_c} f\left(w_c\right) \tag{1}$$

$$f(w) = \left[1 + \left(\frac{c_1 w}{w_c}\right)^3\right] \exp\left(-\frac{c_2 w}{w_c}\right) \tag{2}$$

$$w_c = 5.14 \frac{G_f}{f_{ctm}} \tag{3}$$

$$G_F = 0.073 f_{cm}^{\ 0.18} \tag{4}$$

Steel materials modeling

For this particular study, ideal bilinear modeling was considered based on the mathematical modeling proposed for performing research papers (Hamicha & Kenea, 2022; Kenea, 2022; Kenea & Feyissa, 2022; Maleki & Bagheri, 2008; Feyissa & Kenea, 2022)–(Megarsa & Kenea, 2022). Table 2 shows the elastic–plastic properties of the steel bar used in the FE simulation.

Table 2 Elastic–plastic material properties used for rebars

Elastic Property			Plastic property	
Modulus of elasticity (MPa)	Density (Kg/m^3)	Poisson's ratio	Yield stress (MPa)	Plastic strain
200,000	7850	0.3	533	0
			549	0.0075

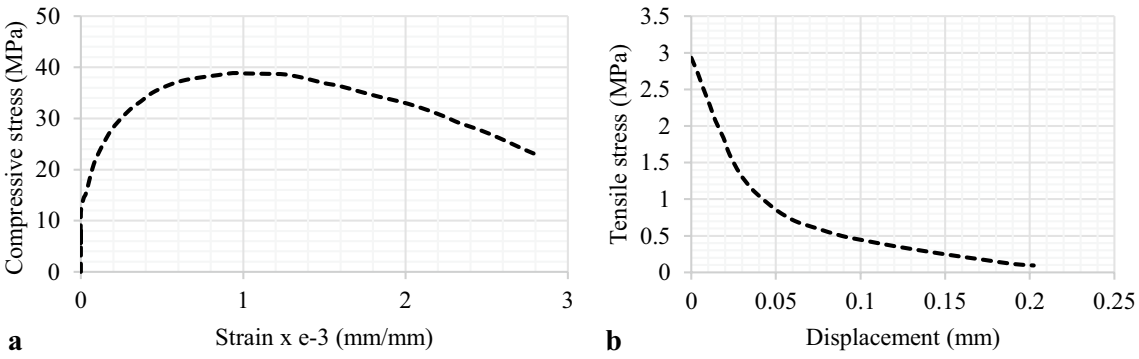

Fig. 1 Sample uniaxial stress–strain curve for C-30.8 **a** Compression and **b** tensile

Geometry and number of specimens

The study considered opening ratio (area of the opening to the face area of the column), eccentricity ratio (eccentricity to the depth of the column), concrete strength, the direction of eccentricity (normal and perpendicular to the longitudinal axis of transverse opening) and position of opening as study variables to investigate the behavior of the RC column. Based on independent variables, 54 RC column specimens were undertaken to access the behavior of columns with the opening at a different position. The RC column with a 150 mm × 150 mm × 700 mm on downscaled dimension was employed. For modeling, four Φ10 mm steel longitudinal reinforcements and six Φ6 mm stirrups with 100 mm center-to-center spacing were used. Table 3 illustrates concentrically loaded column specimens. In another way, Table 4 (eccentricity is parallel to opening) and Table 5 (eccentricity is perpendicular to opening) present eccentrically loaded RC column specimens. The position of the opening was at 0.25H, 0.5H, and 0.75H, which was measured from the top end of the column. The selection of position mainly depends on the high probability of stress concentration at the ends and middle of the column due to maximum shear force and bending moment, respectively. In the designation of the study specimens, the first number represents the position of the opening; the second number represents the magnitude of eccentricity in mm; the third number represents the opening diameter in mm; and the fourth number represents the concrete compressive strength if there.

Analysis step

The analysis procedure is performed using static general, in which 15 mm of displacement is applied axially to perform the parametric study of the modeling. The incremental size in the analysis is fixed initially to 0.001 and increases by a minimum of 1E-015 to a maximum of 1. During analysis, a maximum of 5000 increments was used based on convergence criteria.

Interaction

The interaction between elements of the model is defined through the creation of a constraint sub-option from the interaction module of Abaqus. The created parts include a concrete column, reinforcing steel, stirrups, and an analytical rigid plate. The embedded element option was used to connect the reinforcement and stirrup element to the concrete column host element. The analytical rigid plate is attached to the column using a tie.

Boundary condition and load application

The bottom end of the column is pinned in all directions. The top of the column is pinned in the X and Y directions, allowing for 15 mm of vertical displacement in the Z direction. The analytical rigid plate was used to distribute the applied load effect uniformly over the top end of the column. Figure 2 shows the applied boundary condition of the modeling and the application of displacement in negative Z direction for different cases, where there is no opening

Table 3 Concentrically applied reinforced concrete column model specimens

Direction	Group	Designation	Opening ratio	Eccentricity ratio (e/h)	Concrete strength (Mpa)	Position of opening from top
Load applied concentrically at center of column	G-1	CA1E0π0	0	0	30.8	0.5H
		CA1E0π15	0.1	0	30.8	0.5H
		CA1E0π20	0.133	0	30.8	0.5H
		CA1E0π25	0.167	0	30.8	0.5H
	G-2	CA2E0π15	0.1	0	30.8	0.25H
		CA2E0π20	0.133	0	30.8	0.25H
		CA2E0π25	0.167	0	30.8	0.25H
	G-3	CA3E0π15	0.1	0	30.8	0.75H
		CA3E0π20	0.133	0	30.8	0.75H
		CA3E0π25	0.167	0	30.8	0.75H
	G-4	CA1E0π0-1	0	0	35	0.5H
		CA1E0π0-2	0	0	40	0.5H
		CA1E0π15-1	0.1	0	35	0.5H
		CA1E0π15-2	0.1	0	40	0.5H

Table 4 Models specimens with loading eccentricity parallel to the longitudinal axis of transverse opening

Direction	Group	Designation	Opening ratio	Eccentricity ratio (e/h)	Concrete strength (Mpa)	Position of opening from top
Load applied parallel to longitudinal axis of transverse opening	G-5	CA1E45π0	0	0.3	30.8	0.5H
		CA1E45π15	0.1	0.3	30.8	0.5H
		CA1E45π20	0.133	0.3	30.8	0.5H
		CA1E45π25	0.167	0.3	30.8	0.5H
	G-6	CA1E120π0	0	0.8	30.8	0.5H
		CA1E120π15	0.1	0.8	30.8	0.5H
		CA1E120π20	0.133	0.8	30.8	0.5H
		CA1E120π25	0.167	0.8	30.8	0.5H
	G-7	CA2E45π15	0.1	0.3	30.8	0.25H
		CA2E45π20	0.133	0.3	30.8	0.25H
		CA2E45π25	0.167	0.3	30.8	0.25H
	G-8	CA2E120π15	0.1	0.8	30.8	0.25H
		CA2E120π20	0.133	0.8	30.8	0.25H
		CA2E120π25	0.167	0.8	30.8	0.25H
	G-9	CA3E45π15	0.1	0.3	30.8	0.75H
		CA3E45π20	0.133	0.3	30.8	0.75H
		CA3E45π25	0.167	0.3	30.8	0.75H
	G-10	CA3E120π15	0.1	0.8	30.8	0.75H
		CA3E120π20	0.133	0.8	30.8	0.75H
		CA3E120π25	0.167	0.8	30.8	0.75H
	G-11	CA1E45π15-1	0.1	0.3	35	0.5H
		CA1E45π15-2	0.1	0.3	40	0.5H

Table 5 Models specimens with loading eccentricity perpendicular to the longitudinal axis of transverse opening

Direction	Group	Designation	Opening ratio	Eccentricity ratio (e/h)	concrete strength (Mpa)	Position of opening from top
Loading applied perpendicular to the longitudinal axis of transverse opening	G-12	CB1E45π15	0.1	0.3	30.8	0.5H
		CB1E45π20	0.133	0.3	30.8	0.5H
		CB1E45π25	0.167	0.3	30.8	0.5H
	G-13	CB1E120π15	0.1	0.8	30.8	0.5H
		CB1E120π20	0.133	0.8	30.8	0.5H
		CB1E120π25	0.167	0.8	30.8	0.5H
	G-14	CB2E45π15	0.1	0.3	30.8	0.25H
		CB2E45π20	0.133	0.3	30.8	0.25H
		CB2E45π25	0.167	0.3	30.8	0.25H
	G-15	CB2E120π15	0.1	0.8	30.8	0.25H
		CB2E120π20	0.133	0.8	30.8	0.25H
		CB2E120π25	0.167	0.8	30.8	0.25H
	G-16	CB3E45π15	0.1	0.3	30.8	0.75H
		CB3E45π20	0.133	0.3	30.8	0.75H
		CB3E45π25	0.167	0.3	30.8	0.75H
	G-17	CB3E120π15	0.1	0.8	30.8	0.75H
		CB3E120π20	0.133	0.8	30.8	0.75H
		CB3E120π25	0.167	0.8	30.8	0.75H

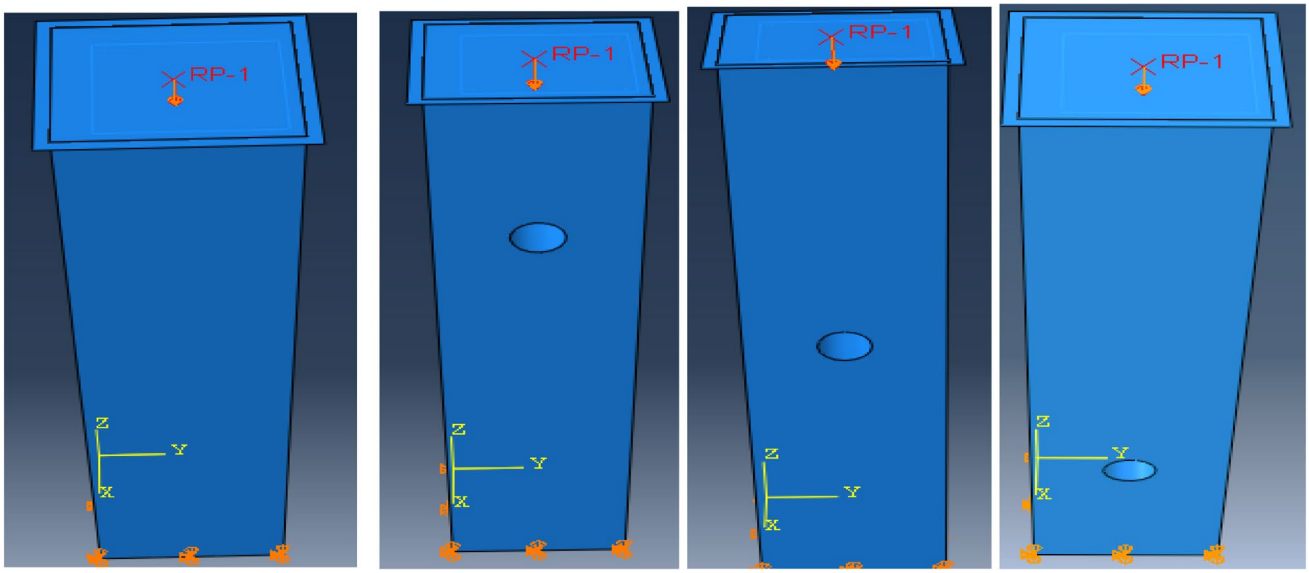

Fig. 2 Boundary condition and application of load with and with out transverse opening

(solid), openings at 0.25H,0.5H, and 0.75H osf the column height from the top to end.

Meshing

The mesh size affects the accuracy of the results obtained from the finite element simulations. The mesh size is selected to give sufficient accuracy and not to make the run time too long. After conducting many trial runs using different finite element mesh sizes, sufficient accuracy was obtained by the 15 mm mesh size and then selected for this study. The concrete column was modeled using eight-node linear brick reduced integration with C3D8R. The reinforcing bars and stirrups were modeled using two-node linear 3-D truss elements with T3D2. Figure 3 illustrates

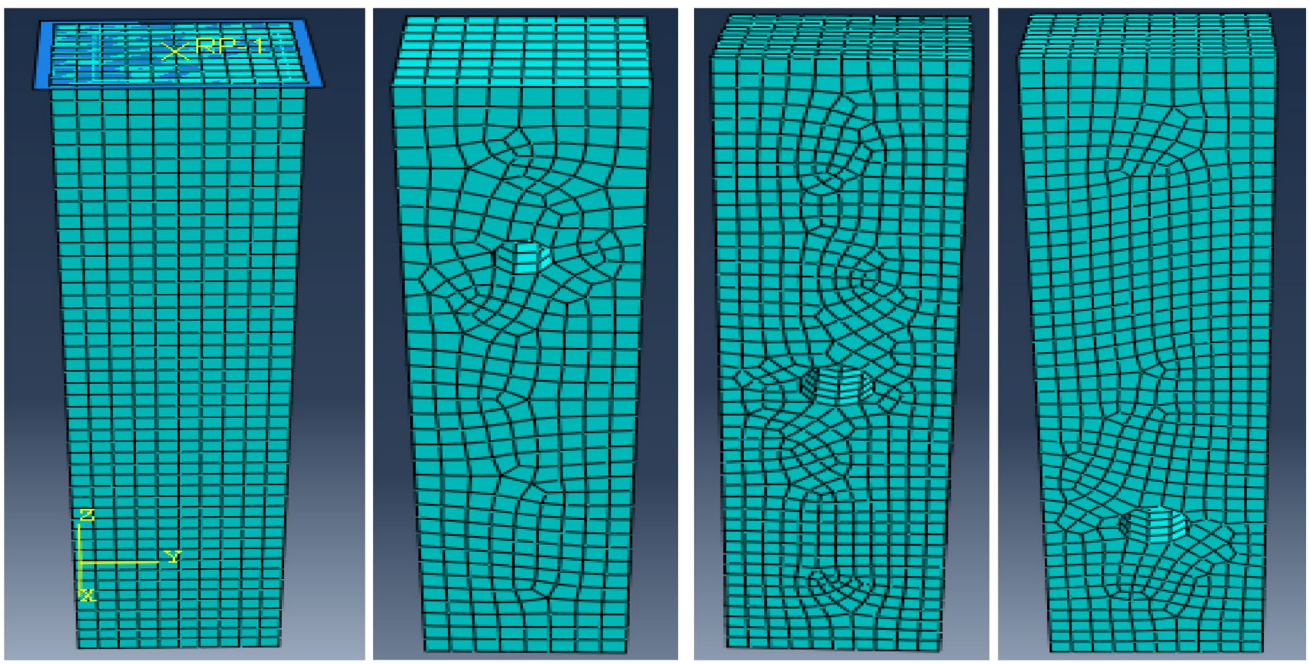

Fig. 3 Meshing of concrete column with and without transverse openings

the concrete column meshed in the FE simulation with and without open.

FE validation

The reliability and accuracy of the finite element model were validated against a previously performed experimental investigation (I. A. S. AL-Shaarbaf, 2017). Two experimental specimens have been selected to evaluate the accuracy of the FE result against the experimental result, by considering columns with and without transverse opening. All conditions (boundary conditions, loading, material properties, and others) considered in the experimental study are accurately applied for the FE modeling. The ultimate load comparison between the FE simulation and experimental results with and without transverse opening in the model is shown in Figure. 4 and Table 6. The result obtained from the FE simulation showed good agreement with the experimental result.

Table 6 Ultimate load comparison between FE and experimental result with and without opening

Model	Figure 4	Experimental result (kN)	FE result (kN)	Percentage of variation
CA1E0π0	(a)	1034.1	964.62	6.7%
CA1E45π25	(b)	400	404.21	1.05%

Result and discussion

Load–displacement curve

Concentrically loaded column

Under this category, the axial load is applied at the center of the column by considering different opening ratios and positions of opening. Figure 5 illustrates a sample of the axial load versus vertical displacement curve of a concentrically loaded column specimen using the opening ratio and position of opening as study parameters. The load versus displacement curves are almost the same for all study specimen's that is why a sample specimen has been selected and shown. The peak point of the curve is significantly decreased as the size of the opening or opening ratio increases. In addition, the peak load was reduced more when the position of the opening was at 0.25H and 0.75H as compared to 0.5H.

Eccentrically loaded column

(a) Eccentricity parallel to transverse opening The behavior of the RC column with the transverse opening was also investigated by considering the load eccentricity effect, which is parallel to the longitudinal axis of the transverse opening. Figure 6 shows a sample of the axial load versus vertical displacement of eccentrically loaded column specimens with different eccentricities, the position of opening and opening ratio as study parameters. As the opening ratio and eccentricity increase, the ultimate or maximum point of the curve is reduced. An opening has a significant effect on the axial load capacity of the RC column when the position of the opening is at 0.25H and 0.75H as compared to the position of the opening at 0.5H.

(b) Eccentricity normal to transverse opening Furthermore, finite element simulation was undertaken to access the axial load-carrying capacity of RC column specimens with different load eccentricities perpendicular to the longitudinal axis of the transverse opening. The axial load versus vertical displacement response of the RC columns was presented in

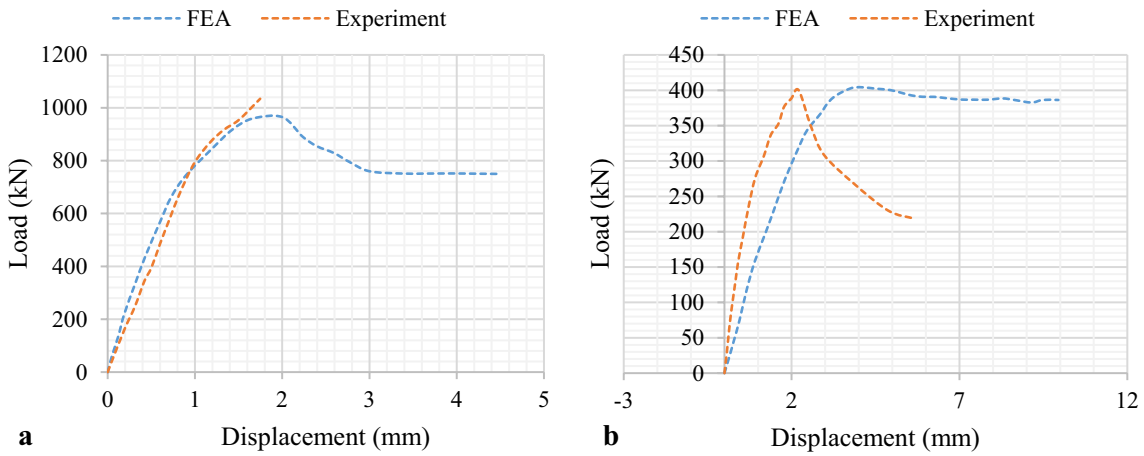

Fig. 4 Comparsion between FE and experimental result **a** CA1E0π0 and **b** CA1E45π25

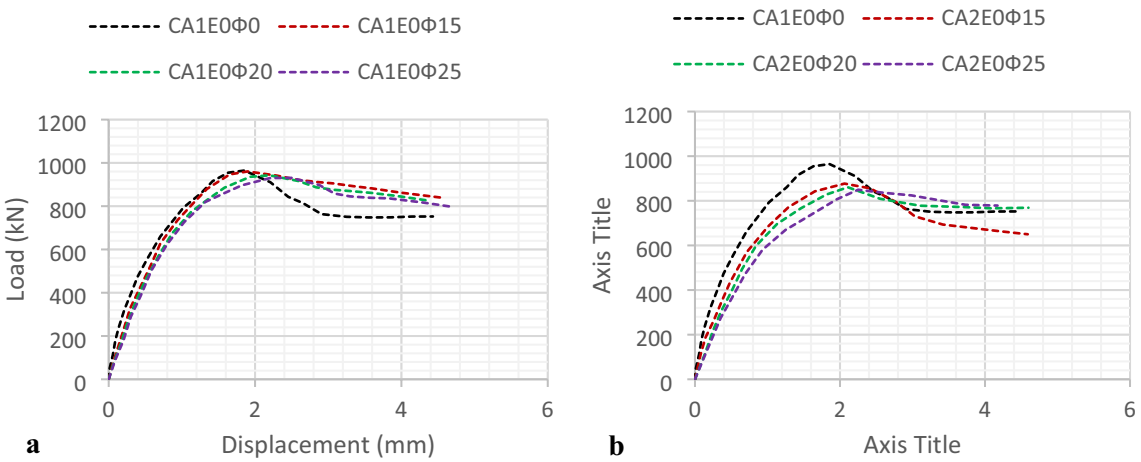

Fig. 5 The load versus vertical displacement curve of concentrically loaded RC column models under different opening ratio

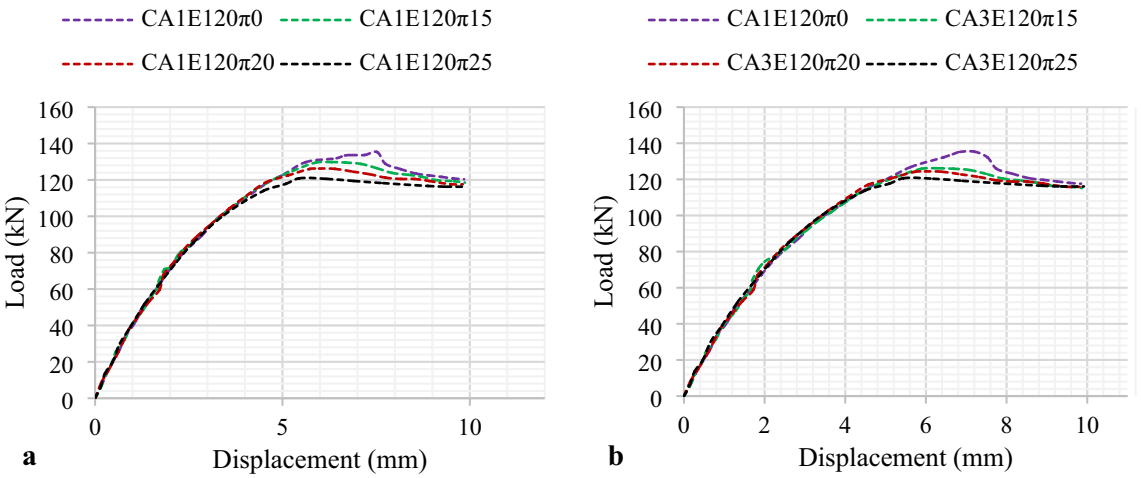

Fig. 6 The load versus vertical displacement curve of eccentrically loaded RC column models under different opening ratio (when eccentricity is parallel to the longitudinal axis of the column)

Figure. 7, by taking the effect of the magnitude of eccentricity and opening ratio into account. The curves have almost the same response at some initial loading stage but are significantly affected by further loading, which results in a tremendous reduction in the maximum point of the curve. Therefore, the axial load capacity is decreased as the opening ratio and eccentricity increase, and vice versa.

Parametric effect on the ultimate strength

Effect of opening ratio

The effect of the opening ratio on the ultimate load capacity of the RC column has been investigated for both concentrically and eccentrically loaded columns under different eccentricities, parallel and normal to the longitudinal axis of the transverse opening. Figure 8 shows the normalized peak load versus the opening ratio of the concentrically loaded (e = 0 mm) column by considering the different positions of opening (@ 0.25H, @ 0.5H, and @ 0.75H), which is measured from the top end of the column. In addition, Fig. 9(a) and Fig. 9(b) illustrate the normalized peak load versus opening ratio of eccentrically loaded ($e/h = 0.3$ or $e = 45$ mm) RC column when the eccentricity is parallel and normal to the longitudinal axis of the opening, respectively, by considering different position of opening (@ 0.25H, @ 0.5H, and @ 0.75H). Figure 10(a), (b) show the normalized peak load versus opening ratio of an eccentrically loaded ($e/h = 0.8$ or $e = 120$ mm) RC column when the eccentricity is parallel and normal to the longitudinal axis of the transverse opening at different opening positions (@ 0.25H, @ 0.5H, and @ 0.75H). The normalized peak load

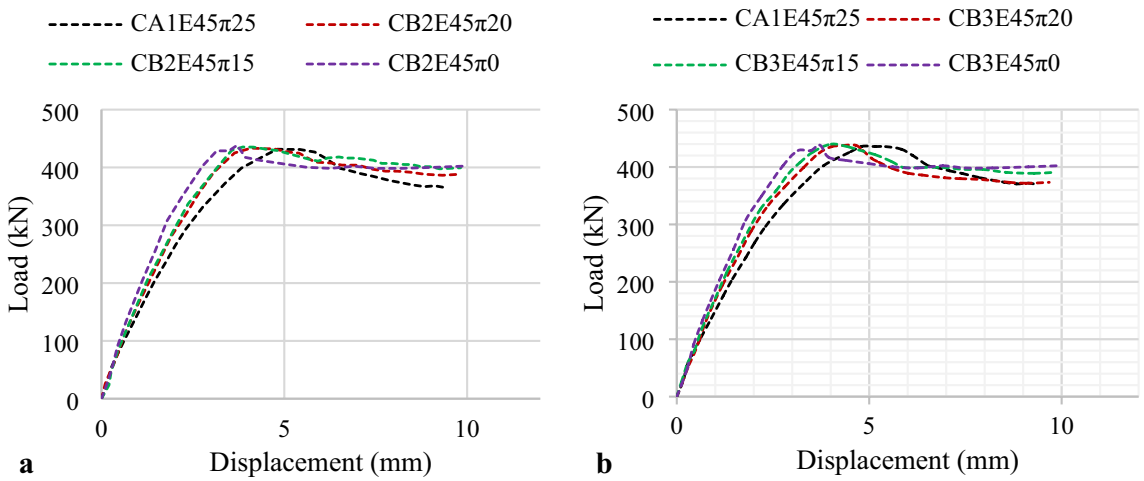

Fig. 7 The load versus vertical displacement curve of eccentrically loaded RC column models under different opening ratio (when eccentricity is normal to the longitudinal axis of the column)

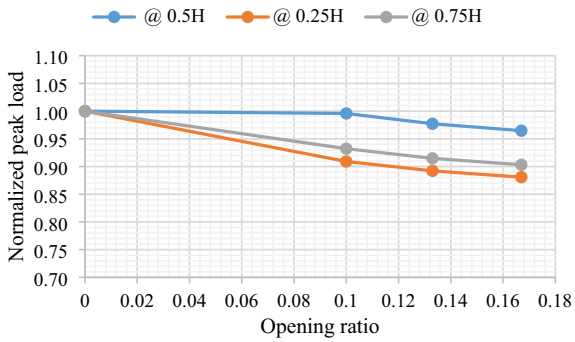

Fig. 8 Normalized peak load versus opening ratio for concentrically loaded columns with e = 0 mm ($e/h = 0$) at different locations

was obtained from the ratio of the ultimate load of each column with different opening ratios to the respective peak load of the column with zero opening ratio. From the results, it is easy to conclude that, as the opening ratio increased, the ultimate or peak load significantly decreased. Therefore, the effect of the opening should be considered during the design of the RC column to be safe under any loading. The ultimate peak load of the concentrically loaded model specimens was decreased by up to 11.92% as the opening ratio increased from 0 to 0.167. When the load is applied with an eccentricity of 45 mm ($e/h = 0.3$), the ultimate load capacity of the model specimens is decreased by up to 20.1% (when the eccentricity is parallel to the opening) and 15.59% (when the eccentricity is perpendicular to the opening) as the opening ratio increases from 0 to 0.167. Further, when the load is applied with an eccentricity of 120 mm ($e/h = 0.8$) that is parallel and normal to the longitudinal axis of the opening, the ultimate load of the model specimens is decreased by up to 12.03% (when the eccentricity is parallel to the opening) and 9.62% (when the eccentricity is perpendicular to the opening) as the opening ratio increases from 0 to 0.167.

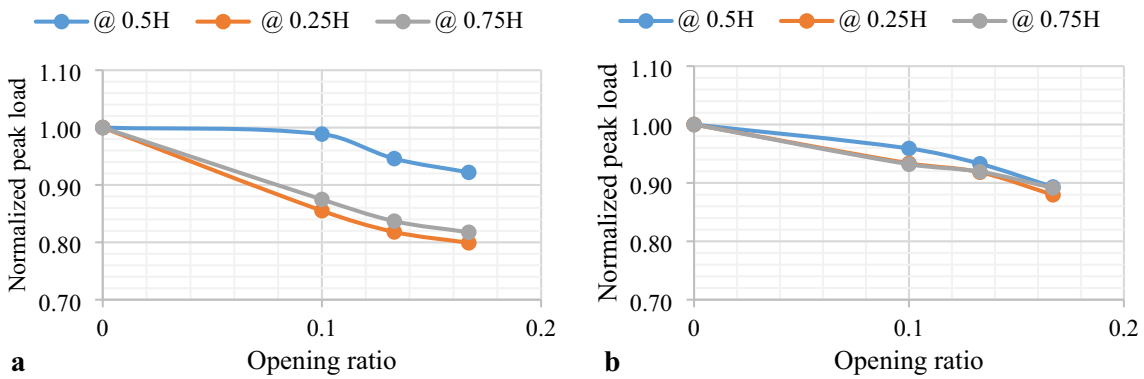

Fig. 9 Normalized peak load versus opening ratio for eccentrically loaded columns with e = 45 mm ($e/h = 0.3$) at different locations [**a** Eccentricity parallel and **b** Eccentricity normal to the longitudinal axis of the opening]

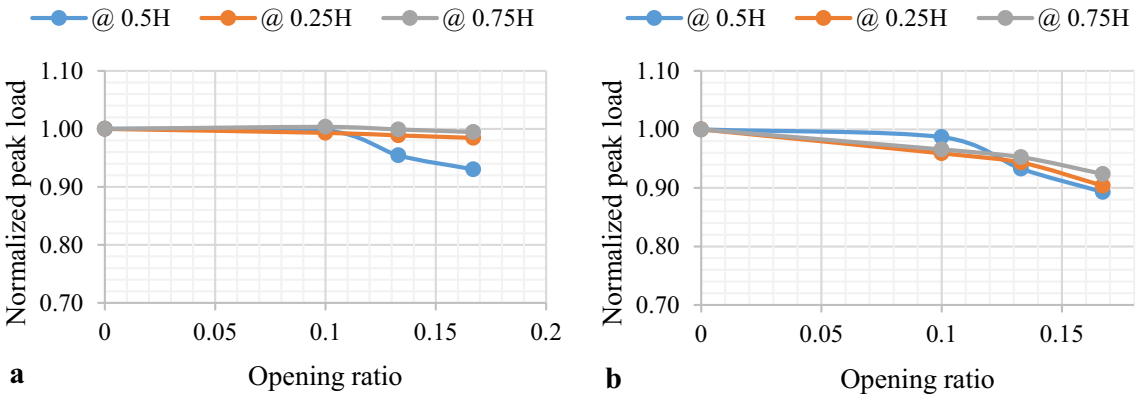

Fig. 10 Normalized peak load versus opening ratio for eccentrically loaded columns with $e = 120$ mm ($e/h = 0.8$) at different locations [**a** Eccentricity parallel and **b** Eccentricity normal to longitudinal axis of the opening]

Effect of eccentricity

In this study, eccentricity was considered as a study parameter to investigate or access its effect on the ultimate load capacity of the RC column with different positions of opening and direction of eccentricity. The study identified the significant effect of eccentricity and its direction with respect to the longitudinal axis of opening on the ultimate load resistance of the RC column.

Figure 11 presents the ultimate load resistance of RC column specimens with different eccentricities (0 mm, 45 mm, & 120 mm) for different opening ratios (0, 0.1, 0.133, & 1.67) and position of opening when the direction of eccentricity is parallel to the longitudinal axis of the transverse opening. As eccentricity parallel to the longitudinal axis of the opening is increased from 0 to 120 mm or ($e/h = 0$ to $e/h = 0.8$), the ultimate load capacity of the models decreased by 87.89%, 83.52%, and 87.65% on average, when the position of the opening is at 0.25H, 0.5H, and 0.75H, respectively**.** Figure 12 presents the ultimate load resistance of the model specimens with different eccentricities (0 mm, 45 mm, & 120 mm) for different opening ratios (0, 0.1, 0.133, & 1.67) and position of opening when the direction of eccentricity is perpendicular to the longitudinal axis of the transverse opening. When the position of opening is at 0.25H, 0.5H, or 0.75H, the ultimate load capacity

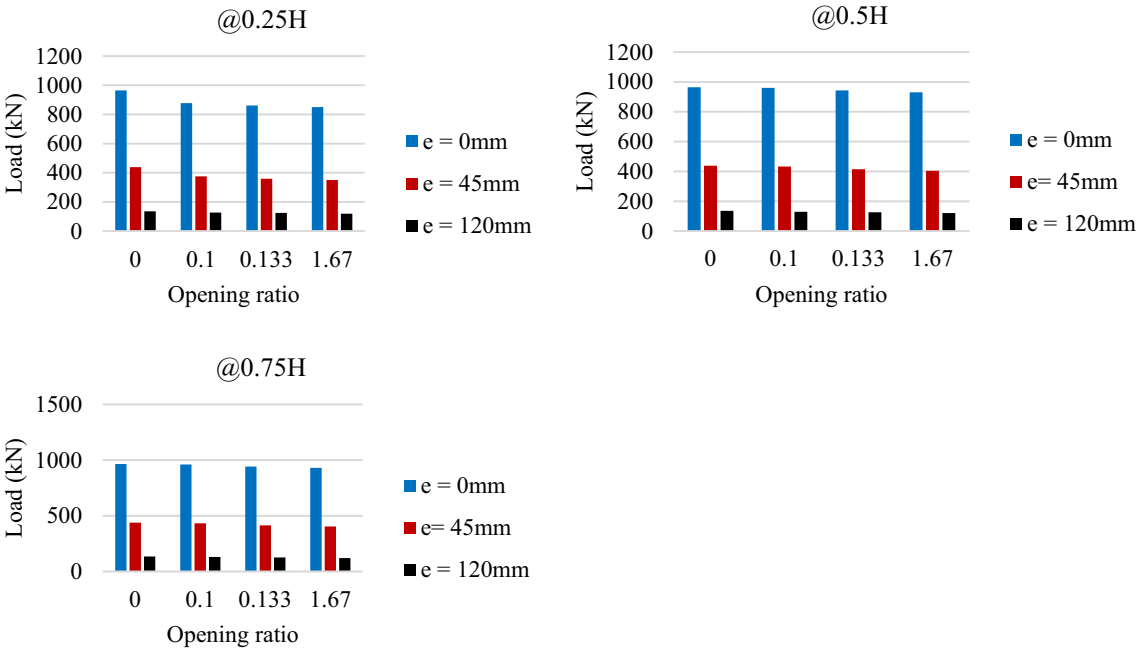

Fig. 11 Effect of eccentricity on the ultimate load capacity when the load eccentricity is parallel to the longitudinal axis of the opening

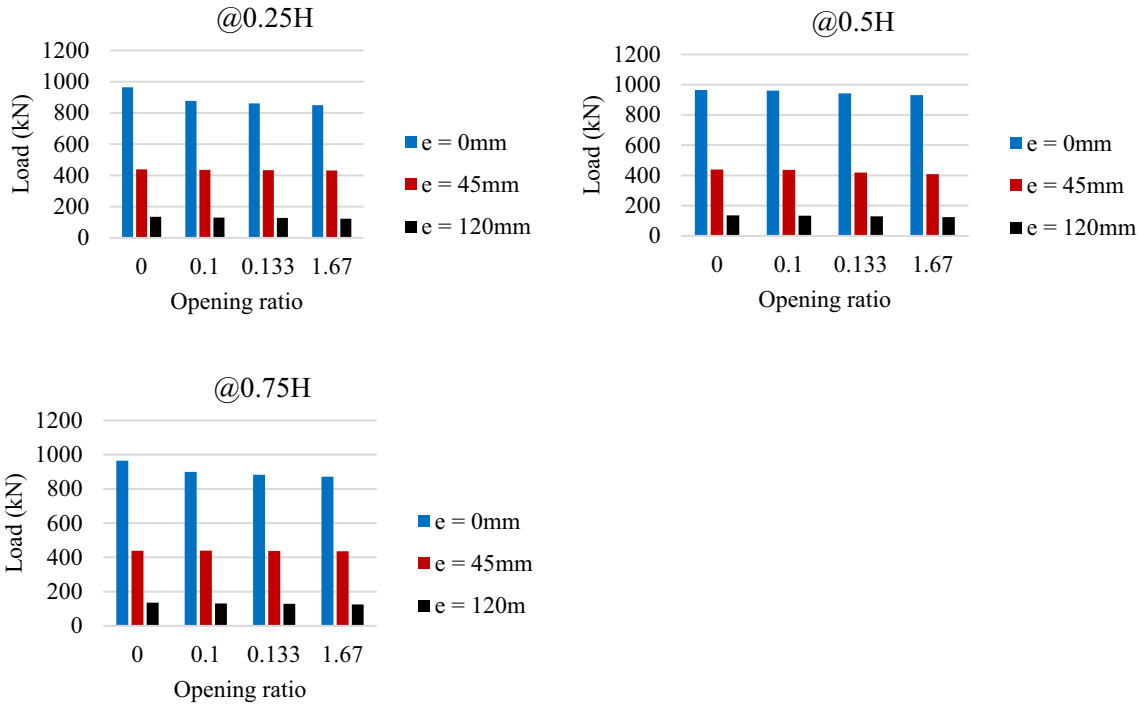

Fig. 12 Effect of eccentricity on the ultimate load capacity when the load eccentricity is normal to the longitudinal axis of the opening

of the models decreases by 85.73%, 81.51%, and 86.01% on average as the eccentricity increases from 0 to 120 mm or ($e/h = 0$ to $e/h = 0.8$). This implies that the eccentricity has a significant effect on the ultimate capacity of the column, which is caused by the increasing bending moment due to the increase in eccentricity.

Effect of concrete strength

Keeping other parameters constant, the effects of concrete grade on ultimate load resistance of RC columns have been investigated by considering transverse openings. Figure 13(a) depicts the load versus vertical displacement curve of RC column specimens with concentrically applied and no transverse opening under different concrete strengths (30.8 Mpa, 35 Mpa, and 45 Mpa). As concrete strength increased from 30.8 Mpa to 40 Mpa, the ultimate load capacity of the RC column increased by 22.90%. The load versus vertical displacement response of RC column specimens with an e/h of 0 and an opening ratio of 0.1 with different concrete strengths (30.8 Mpa, 35 Mpa, and 45 Mpa) is shown in Figure. 13(b). The ultimate load capacity is increased by 22.3% when the concrete strength is increased from 30.8Mpa to 40Mpa. Figure 13(c) shows the load versus vertical displacement response of RC column specimens with an e/h of 0.3 and an opening ratio of 0.1 in three different concrete strengths (30.8 Mpa, 35 Mpa, and 45 Mpa). The ultimate load capacity is increased by 27.4% when the concrete strength is increased from 30.8Mpa to 40Mpa. The specimens in each curve have almost the same response to initial load increment, which is significantly affected by further load increment. This implies that as concrete strength increases, the ultimate load resistance also increases. Therefore, the effect of transverse opening on the load-carrying capacity of the concrete column is significantly minimized using concrete with high compressive strength.

Effect of location of opening

In this research, the analysis was done by providing openings at different locations over the height of the reinforced concrete column. Three opening positions were selected, which were located at 0.25H, 0.5H, and 0.75H when measured from the top end of the column. From the analysis, it is concluded that the effect of the position of openings slightly affects the load-carrying capacity of the RC column. From the total results of the FE simulation, specimens with an opening position of 0.25H and 0.75H have slightly a lower ultimate load capacity than specimens with an opening position of 0.5H. Therefore, the ultimate load capacity of the RC column is reduced more when an opening is provided at 0.25H or 0.75H from the top end of the column. Therefore, during the analysis and design of reinforced concrete columns, the effect of the position of the opening should be incorporated to have a safe designed column structure. In a frame structure, the combined effect of shear and bending

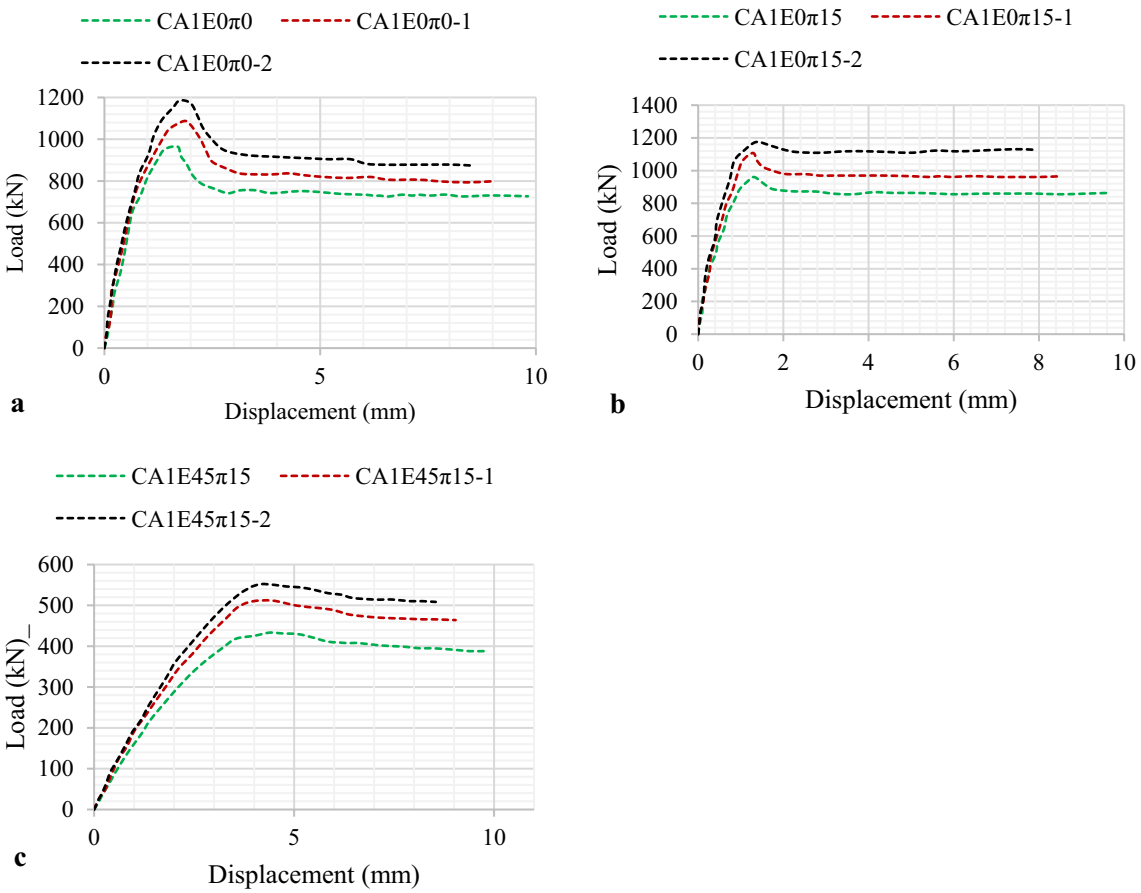

Fig. 13 Effect of concrete strength on the ultimate strength of RC column with concentrically and eccentrically loaded in which eccentricity is parallel to longitudinal axis of the opening

moment is mostly located at the top end or bottom end of the column. This is in addition to the axial load has a significant effect when combined with the location of opening in the column. There is a direct relationship between the bending moment and eccentricity. From this study, it is concluded that providing an opening at 0.5H of the column allows a higher performance under the combined action of axial load and bending moment.

Damaging mode

Damage or failure mode allows identifying the most affected region of the model specimens based on the stress concentration. Since the damage mode of all specimens was almost similar, a certain number of specimens were undertaken by considering the different position of opening, opening ratio, and eccentricity ratio for both compressive and tensile damage. Non-uniformity in stress concentration may be caused by a type of loading, and geometric condition of the specimens. Figure 14, Figure. 15, Figure. 16, and Figure. 17, Figure. 18 illustrate the compression damage mode and compressive damage versus strain of CA1E45π15, CA1E45π20, and CA1E45π25, respectively. In another way, Figure. 12, Figure. 14, and Figure. 16 present the tensile damage mode and tension damage versus displacement of CA1E45π15, CA1E45π20, Figure. 19 and CA1E45π25, respectively. The study revealed that there is a high-stress concentration around the opening due to geometric discontinuity. Therefore, elements around the opening are more affected than other regions of the model.

As the diameter of the opening increases, a large portion (more elements) of the RC column are damaged by compression and tension around the transverse opening. The highlighted part of the column is more affected due to tension and compression damage. As it can be seen from the contour visualization, the parts of the reinforced concrete column around openings are damaged due to compression and tension stress concentration. As the diameter of the opening increases, wide parts of concrete columns are damaged by compression and tension.

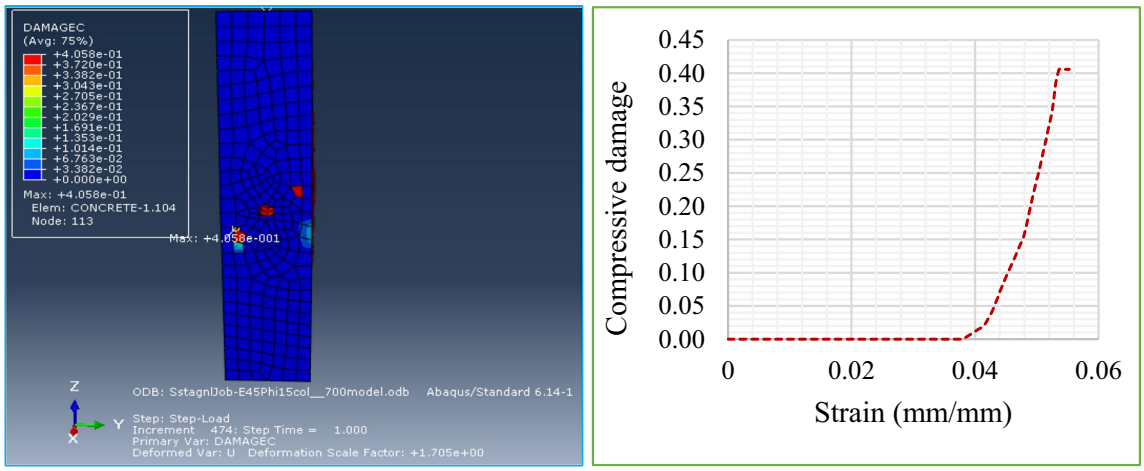

Fig. 14 **a** Compressive damage and **b** Compressive damage versus strain curve for CA1E45π15 with opening position at 0.5H

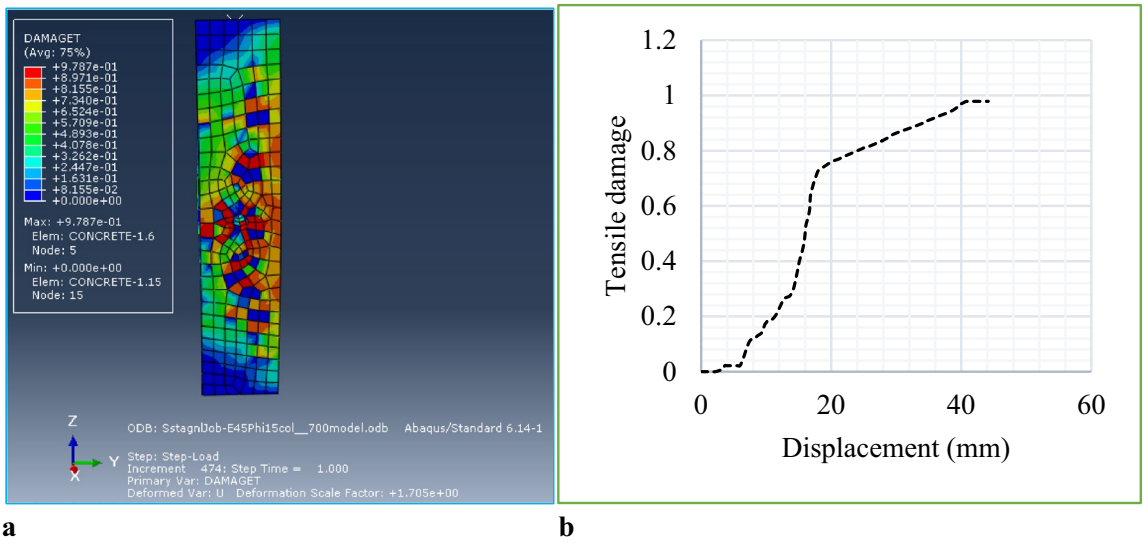

Fig. 15 **a** Tensile damage and **b** Tensile damage versus displacement curve for CA1E45π15 with opening position at 0.5H

Sensitivity analysis

Sensitivity analysis is very important to identify how much each independent variable effects the dependent variable or output. Based on this necessity, an extensive multi-linear regression has been conducted in the SPSS software package using input and output data from FE simulation. The study considered the combined effect of independent variables on the ultimate capacity of the model specimens by a single equation, as presented in Eq. 5.

$$P_{ult} = -1609.96\emptyset_r - 352.1e_{po} - 273.98e_{no} - 12.5l_{po} + 23.0f_{ck} + 121.27 \quad (5)$$

Based on the sign of the coefficient of the independent variable, the ultimate load capacity of model specimens increased as concrete compressive strength increased. However, the ultimate load capacity is decreased as the opening ratio, eccentricity ratio, and position of the opening increase. Some error is observed from the combined variable equation as compared to the result from FE simulation, regarding the position of the opening. Equation 5 shows the ultimate load resistance is decreased as the position of the opening increases. However, the result from the FE simulation showed a minimum ultimate load capacity when the position of the opening is at 0.25H and 0.75H. The comparison reveals the supportive idea at the bottom end of the column (0.75H) and the controversial idea at the top end (0.25H) and

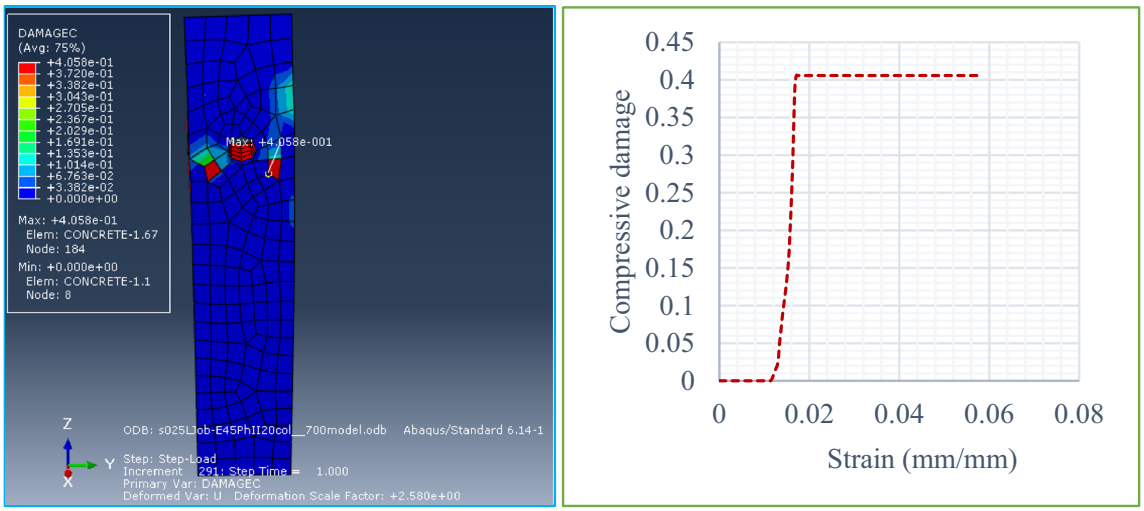

a **b**

Fig. 16 **a** Compressive damage and **b** Compressive damage versus strain curve for CA1E45π20 with opening position at 0.25H

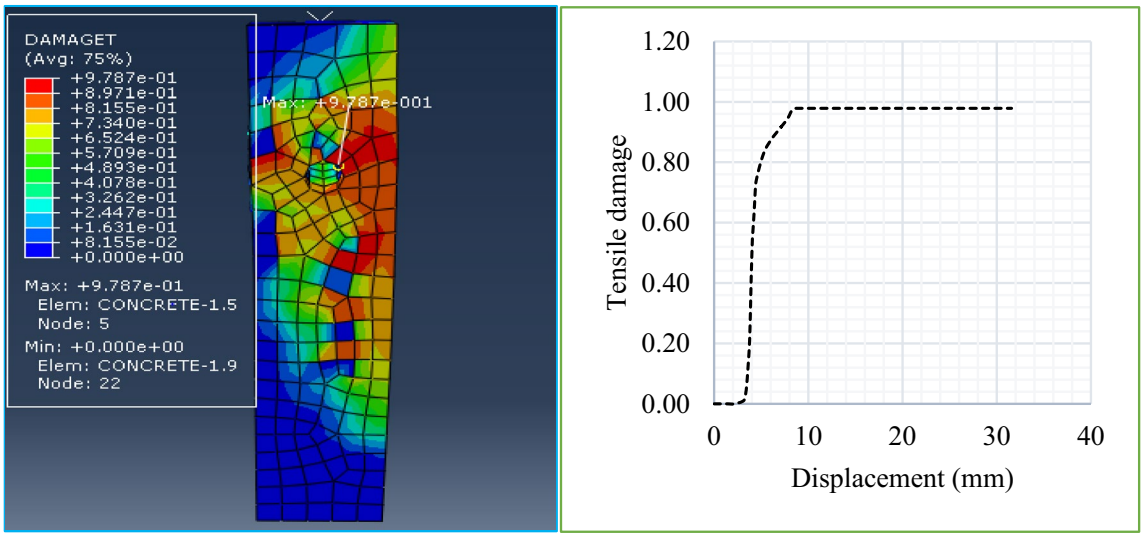

a **b**

Fig. 17 **a** Tensile damage and **b** Tensile damage versus displacement curve for CA1E45π20 with opening position at 0.25H

mid-span (0.5H) of the column. This problem arose because of the linearity of each independent variable in the combined equation.

Conclusion

An intensified non-linear FE analysis has been modeled in Abaqus software to investigate the effect of opening ratio, the position of opening, concrete strength, eccentricity ratio normal and perpendicular to the opening axis on the ultimate

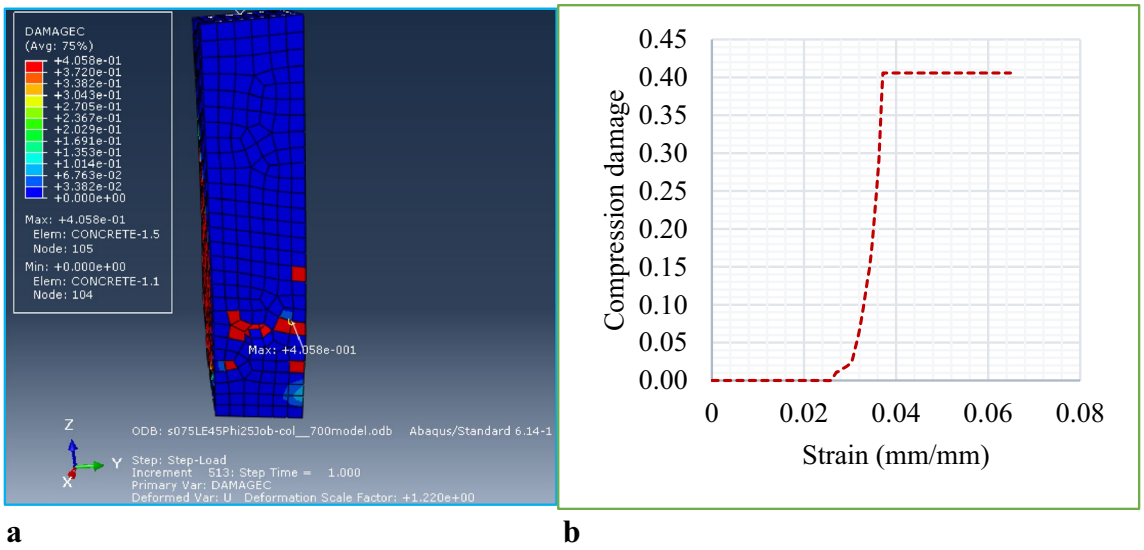

Fig. 18 **a** Compressive damage and **b** Compressive damage versus strain curve for CA1E45π25 with opening position at 0.75H

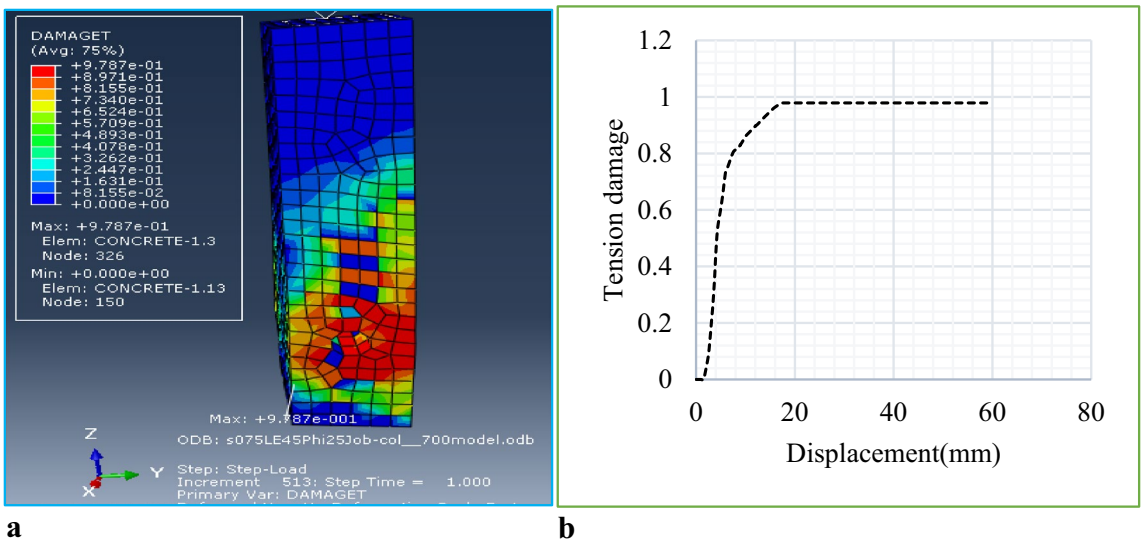

Fig. 19 **a** Tensile damage and **b** Tensile damage versus displacement curve for CA1E45π25 with opening position at 0.75H

load capacity of the reinforced concrete column. The models were validated against a previously performed experimental investigation (I. A. S. AL-Shaarbaf, 2017), which showed a good agreement during comparison of the result. In addition, the damage mode (tensile and compression damage) of the RC column in the presence of an opening has been investigated based on the result from the FE simulation. Furthermore, sensitivity analysis was undertaken to see how much the independent variables affect the ultimate load capacity of the models in individual and combination. Based on the FE simulation result the following conclusion has been drawn:

a) As the opening ratio increased from 0 to 1.67, the ultimate axial load capacity of the RC column model specimens decreased by up to 11.92%, 20.1%, and 15.59% when the loading eccentricity ratio became 0, 0.3, and 0.8, respectively.
b) The study revealed that the loading eccentricity has a significant effect on the axial load capacity of the RC column. The ultimate load capacity of the models decreased by 44.7% (when the opening is parallel) and 42.6% (when the opening is perpendicular) on average as the eccentricity ratio increased from $e/h = 0$ to $e/h = 0.8$.

c) The ultimate axial load capacity of the RC column is more reduced when the position of the opening is provided at 0.25H and 0.75H from the top end compared to the position of opening at 0.5H.
d) In addition, the study confirmed the tremendous effect of concrete compressive strength on the axial load capacity of the RC column model. The ultimate axial load capacity of the model specimens increased up to 27.4%, as the concrete compressive strength increased from 30.8Mpa to 40Mpa.
e) Further, the concrete damage has been analyzed to access the failure mode of the model under axial loading with eccentricity and opening ratio. The finite elements around the opening are highly effected due to stress concentration. As the opening ratio increased, large portion elements were subjected to compressional and tensional damage due to geometric discontinuity.

Acknowledgements The authors would like thank all those who stand with us by giving advising and time to review the paper.

Funding There is no funding source for this particular study.

Data availability statement All the required data are available in the manuscript.

Declarations

Conflict of interest The authors declare that there is no conflict of interest regarding to the paper.

References

A. C. I. (2014) Committee, Building Code Requirements for Structural Concrete (ACI 318–14) An ACI Standard. Commentary on Building Code Requirements for Structural Concrete (ACI 318R-14). Farmington Hills, MI, USA: American Concrete Institute: Farmington Hills, MI, USA

Abdullah, K. T. A. (2000). "Experimental Study on reinforced concrete column strengthened with Ferro cement Jacket", in 12WCEE. *Journal of Physics: Conference Series, 1624*(4), 1–8. https://doi.org/10.1088/1742-6596/1624/4/042078

Alfarah, B., López-almansa, F., & Oller, S. (2017). New methodology for calculating damage variables evolution in Plastic Damage Model for RC structures. *Engineering Structures, 132*, 70–86. https://doi.org/10.1016/j.engstruct.2016.11.022

Al-Maliki, H. N. G., Alshimmeri, A. J. H., Ali, A. M., Madhloom, H. M., & Gamil, Y. (2021). Nonlinear simulation analysis of tapered reinforced concrete column (solid and hollow) behavior under axial load. *Geomate Journal, 21*(86), 131–146. https://doi.org/10.21660/2021.86.j2295

Bakhteri, J., & Iskandar, S. A. (2005). Experimental study of reinforced concrete columns concealing rain water pipe. *Jurnal Teknologi, 43*(1), 13–26. https://doi.org/10.11113/jt.v43.763

Balanji, E. K. Z., Sheikh, M. N., & Hadi, M. N. S. (2016). Performance of high strength concrete columns reinforced with hybrid steel fiber under different loading conditions. *Proceedings of International Structural Engineering and Construction, 3*(1), 35–40. https://doi.org/10.14455/ISEC.res.2016.83

Cornelissen, H. W., Hordijk, D. A., & Reinhardt, H. (1986). Experimental determination of crack softening characteristics of normal weight and lightweight concrete. *Mater Science, 31*(2), 45.

European Committee for Standardization, (2002) Eurocode 2: Design of concrete structures - Part 1: General rules and rules for buildings, vol. 1, no. November. Brussels: European Committee for Standardization,.

Feyissa, A., & Kenea, G. (2022). Performance of shear connector in composite slab and steel beam with reentrant and open trough profiled steel sheeting. *Advances in Civil Engineering, 2022*, 1–14.

Gholipour, G., Zhang, C., & Mousavi, A. A. (2020). Numerical analysis of axially loaded RC columns subjected to the combination of impact and blast loads. *Engineering Structures, 219*, 110924. https://doi.org/10.1016/j.engstruct.2020.110924

Hamicha, A., & Kenea, G. (2022). 2022 "Investigation on the effect of geometric parameter on reinforced concrete exterior shear wall-slab connection using finite element analysis." *Advances in Civil Engineering, 1*, 17.

Hassan, R. F., Sarsam, K. F., & Allawi, A. A. E. (2013). Behavior of strengthened RC columns with CFRP under biaxial bending. *J. Eng., 19*(9), 1115–1126.

Hoshikuma, J. I., & Priestley, M. J. N. (2000). Flexural behavior of circular hollow columns with a single layer of reinforcement under seismic loading. *Ssrp, 59*, iii–79.

Hwang, Y. H., Yang, K. H., Mun, J. H., & Kwon, S. J. (2020). Axial performance of RC columns strengthened with different jacketing methods. *Engineering Structures, 206*, 110179. https://doi.org/10.1016/j.engstruct.2020.110179

A. Ibrahim, M. Al-osta, and R. Hindi, 2015 "Numerical investigation of reinforced concrete columns with opposing spirals under axial compression loads," SMAR 2015 - Third Conf. Smart Monit. Asseesment Rehabil. Ciivil Struct. pp. 1–8

A. Inc, "ABAQUS Version 6.10–1 Analysis User's Manual," Dassault Systèmes Simulia Corp., vol. III, pp. 1–10, 2017, [Online]. Available: http://130.149.89.49:2080/v6.10/pdf_books/ANALYSIS_3.pdf%0Ahttp://www.simulia.com/products/%0Ahttp://130.149.89.49:2080/v6.10/pdf_books/ANALYSIS_3.pdf%0Ahttp://www.simulia.com/products/

Isleem, H. F., et al. (2021). Axial compressive strength models of eccentrically-loaded rectangular reinforced concrete columns confined with frp. *Materials (basel), 14*(13), 3498. https://doi.org/10.3390/ma14133498

Jiang, C., & Wu, Y. F. (2020). Axial strength of eccentrically loaded FRP-confined short concrete columns. *Polymers (basel), 12*(6), 32–41. https://doi.org/10.3390/POLYM12061261

Karihaloo, B. L., Abdalla, H. M., & Imjai, T. (2003). A simple method for determining the true specific fracture energy of concrete. *Magazine of Concrete Research, 55*(5), 471–481. https://doi.org/10.1680/macr.2003.55.5.471

Kenea, G. (2022). Analytical study of geometric parameter effect on the behavior of horizontally curved reinforced concrete deep beam. *Journal of Engineering, 2022*, 1–14. https://doi.org/10.1155/2022/8052852

Kenea, G., & Feyissa, A. (2022). Cyclic behavior of reinforced concrete slab-column connection using numerical simulation. *Advances in Civil Engineering, 2022*, 1–14. https://doi.org/10.1155/2022/2814715

Khelil, A., Boissière, R., Mahmoud, F. A., Wurtzer, F., & Blin-Lacroix, J. L. (2015). Experimental and numerical investigation on axial compression of reinforced concrete columns made from recycled coarse and fine aggregates. *Structural Concrete, 22*, 1–14. https://doi.org/10.1002/suco.202000035

Khelil, A., Boissière, R., Al Mahmoud, F., Wurtzer, F., & Blin-Lacroix, J. L. (2021). Numerical investigation for the structural behaviour

for partially-loaded high strength concrete columns under uniaxial loading. *Kerbala Journal for Engineering Science, 22*(S1), E193–E206. https://doi.org/10.1002/suco.202000035

Krainskyi, P., Blikharskyy, Y., Khmil, R., & Blikharskyy, Z. (2018). Experimental study of the strengthening effect of reinforced concrete columns jacketed under service load level. *MATEC Web of Conferences, 183*, 4. https://doi.org/10.1051/matecconf/201818302008

Landović, A., & Bešević, M. (2021). Experimental research on reinforced concrete columns strengthened with steel jacket and concrete infill. *Applied Sciences, 11*(9), 4043. https://doi.org/10.3390/app11094043

Li, X., Zhang, R., Jin, L., & Du, X. (2021). Numerical analysis of axial compressive behavior of RC short columns subjected to non-uniform fire: A meso-scale study. *E3S Web of Conferences, 272*, 1–5. https://doi.org/10.1051/e3sconf/202127202028

Maleki, S., & Bagheri, S. (2008). Behavior of channel shear connectors, Part II: Analytical study. *Journal of Constructional Steel Research, 64*(12), 1341–1348. https://doi.org/10.1016/j.jcsr.2008.01.006

Megarsa, E., & Kenea, G. (2022). 2022 "Numerical investigation on shear performance of reinforced concrete beam by using ferrocement composite." *Mathematical Problems in Engineering., 1*, 12.

Othman, Z. S., & Mohammad, A. H. (2019). Behaviour of eccentric concrete columns reinforced with carbon fibre-reinforced polymer bars. *Advances in Civil Engineering, 2019*, 1–13. https://doi.org/10.1155/2019/1769212

Raza, A., et al. (2020). Prediction of axial load-carrying capacity of GFRP-reinforced concrete columns through artificial neural networks. *Structures, 28*, 1557–1571. https://doi.org/10.1016/j.istruc.2020.10.010

Rodrigues, E. A., Manzoli, O. L., Bitencourt, L. A. G., dos Prazeres, P. G. C., & Bittencourt, T. N. (2015). Failure behavior modeling of slender reinforced concrete columns subjected to eccentric load. *Latin American Journal of Solids and Structures, 12*(3), 520–541. https://doi.org/10.1590/1679-78251224

Shaarbaf, I. A. S. A. L., Allawi, A. A., & AlSalim, N. H. (2017). Strength of reinforced concrete columns with transverse openings. *Journal of Engineering, 23*(10), 114–133.

Son, K., Pilakoutas, K., & Neocleous, K. (2006). Behaviour of concrete columns with drilled holes. *Magazine of Concrete Research, 9831*(7), 411–419.

Waryosh, W. A., Rasheed, M. M., AL-musawi A. H. (2012). Experimental study of reinforced concrete columns strengthened with CFRP under eccentric loading. *Journal of Engineering and Suistainable Development, 16*(3), 421–440.

Yusuf Sümer, M. A. (2015). Defining parameters for concrete damage plasticity model. *Challenge Journal of Structural Mechanics*. https://doi.org/10.20528/cjsmec.2015.07.023

M. Zarei. (2016) "Normal-Strength and High-Strength Concrete Columns Under Cyclic Axial Load And Biaxial Moment,".

Zhang, X., Kunnath, S., & Xiao, Y. (2017). Experimental study of reinforced concrete columns damaged by fire following an earthquake. *Advances in Structural Engineering and Mechanics, 28*, 1–6.